

Unusual magnetic behavior in ferrite hollow nanospheres

E. Lima Jr.*, J. M. Vargas, R. D. Zysler[†]

Centro Atómico Bariloche and Instituto Balseiro, 8400 S. C. de Bariloche, RN, Argentina

H. R. Rechenberg

Instituto de Física, Universidade de São Paulo, 05315-970, São Paulo, SP, Brazil.

J. Arbiol

TEM-MAT Serveis Científico-técnicos, Universidad de Barcelona, 08028, Barcelona, Spain.

G. F. Goya[‡], A. Ibarra, M. R. Ibarra

Instituto de Nanociencia de Aragón, Universidad de Zaragoza, 50009, Zaragoza, Spain.

(Dated: December 4, 2021)

We report unusual magnetic behavior in iron oxide hollow nanospheres of 9.3 nm in diameter. The large fraction of atoms existing at the inner and outer surfaces gives rise to a high magnetic disorder. The overall magnetic behavior can be explained considering the coexistence of a soft superparamagnetic phase and a hard phase corresponding to the highly frustrated cluster-glass like phase at the surface regions.

PACS numbers: 75.50.Tt, 75.50.Gg, 75.50.LK, 75.60.Ej

Keywords: Fine Particles, Superparamagnetism, Magnetic ordering, Magnetic Freezing

Finite size-effect occurs in nanostructured materials as thin films, nanoparticles and nanowires. The control of their morphology and functionalities at the nanoscale is a prerequisite for some biomedical applications that use nanoparticles as nanovectors for drug delivery [1]. Spherical empty nanocapsules are appealing for these applications because they could store larger amounts of drug than solid NPs of the same size. The unique magnetic phenomena reported for core-shell nanoparticles along the last years have been usually assigned to the complex surface microstructure and/or exchange interactions at the core/surface interface [2, 3]. The magnetic behavior of the surface atoms is characterized by the existence of broken symmetry and exchange bonds which introduce structural and magnetic disorder and originate an enhancement of the magnetic anisotropy and the coercive field [4]. On the bases of the huge surface/bulk atomic ratio, Hollow NanoSpheres (HNS) provide an excellent scenario to study the competition between surface and bulk magnetism at nanoscale level and open up new perspectives for theoretical developments. The synthesis of HNS have been recently reported [5], using controlled oxidation of Fe or Fe₃O₄ nanoparticles after synthesis, at temperatures of 473-473 K. In this work we present a different, low-temperature synthesis method for obtaining monodisperse ferrite HNS without need of subsequent oxidation process. The unusual magnetic behavior found

in these particles can be interpreted on the basis of soft and hard phases and the large surface/bulk atomic ratio due to both inner and outer surfaces of a hollow sphere.

Ferrite HNS were prepared by modifications at the high-temperature organic-phase synthesis from the precursor Fe(acac)₃ at phenylether (boiling point ~ 533-543 K) in the presence of a long-chain alcohol (1,2-hexadecanediol) and oleic acid and oleylamine surfactants [6], using a molar ratio precursor:surfactant of 1:9 to control the final diameter of the particles [7]. The synthesis lasted 30 minutes in argon flux (~0.5 L/min.), but differently from those described in the literature, a (noncontrolled) temperature reduction was induced during the synthesis procedure. Final HNS were coated by surfactant molecules, avoiding agglomeration and increasing the chemical stability of the surface. They were further dispersed by dilution in toluene and alcohol dilutes polyethylemine (PEI). After that the solvents were left to evaporate, being stirred from time to time. At the end, HNS dispersed to 5 % wt in PEI were obtained; this dilution is sufficient to ensure a negligible dipolar interaction. The morphology, structure and composition of the particles were studied using High-resolution TEM (HRTEM) combined with Energy Electron Loss Spectroscopy (EELS) and Energy Filtered TEM (EFTEM) as well as high angular annular dark field (HAADF) and Bright Field TEM (BFTEM). The samples were prepared by dropping a colloidal solution of HNS onto a carbon-coated copper grid. Fig. 1-a shows a general view of the sample in which 9.3 nm in diameter nanoparticles are observed. The iron oxide spinel structure obtained from the Fourier transformation of the HRTEM (1-b) images is consistent with that obtained from X-ray diffraction.

*Presently at: Instituto de Física, Universidade de São Paulo, Brazil

[†]corresponding author, e-mail: zysler@cab.cnea.gov.ar

[‡]corresponding author, e-mail: goya@unizar.es

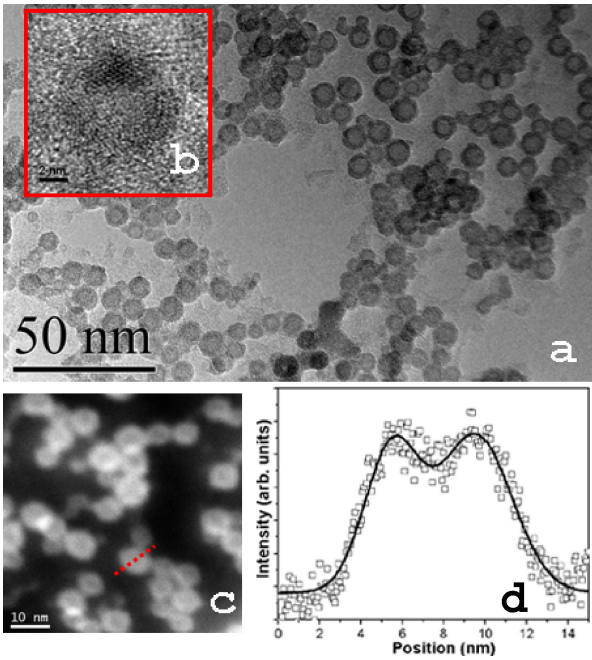


FIG. 1: a) TEM micrograph of the sample where the projection of nanoparticles shows toroidal-like structures of 9.3 nm in diameter, b) HRTEM obtained on one of the nanostructures c) HAADF STEM images and d) STEM profile through one single nanoparticle indicated in c) showing an enhanced contrast at the particle edge.

Furthermore, broadening of the X-ray patterns reflects the existence of crystallite sizes of 2 nm, much lower than the 9.3 nm observed from HRTEM. Detailed analysis of magnified HRTEM revealed the polycrystalline nature of the nanostructures with the absence of any preferential orientation. It is important to point out that depending on the defocus, crystal plains with d-spacing corresponding to spinel structure were observed either on the external part or on the top of the inner part. This discards the existence of toroidal-like structures. EELS and EFTEM analysis (not shown) have revealed that the only elements composing the nanospheres were Fe and O. HAADF (Fig. 1-c) and STEM (Fig. 1-d) analysis denotes a increase of the density at the outer part. All these data reveal that the observed nanoparticles are HNS. Moreover, BFTEM micrograph at high tilt angle (35°) do not show changes on the observed morphology denoting once more that our nanoparticles are HNS. Figure 2 displays the $M(T)$ curves ($H = 20$ Oe) measured in the ZFC and FC (cooling field $H = 20$ Oe). The ZFC results exhibit a sharp peak at ~ 36 K. This temperature coincides with irreversibility temperature (i.e. the temperature above which the ZFC and FC curves coincide). This is a indication of the existence of a very narrow size distribution as observed in Fig. 1-a. Unexpectedly, the ZFC magnetization as the FC magnetization turns up below 20 K. This anomaly occurs at the same temperature range where we observe

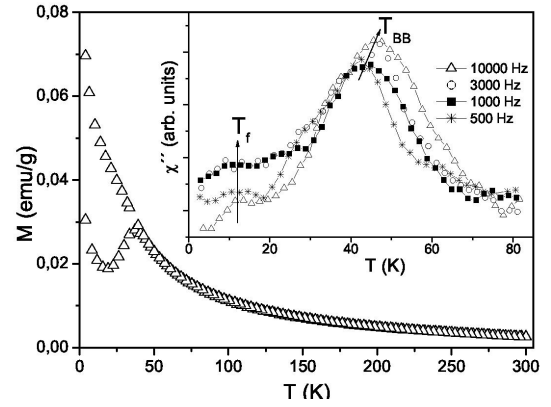


FIG. 2: Magnetization as a function of temperature. All curves are collected from 2 K up to 300 K with applied field of $H = 20$ Oe. ZFC (lower branch) and FC (upper branch) data are shown. Inset: Thermal and frequency dependence of the out-of-phase χ'' component of the ac susceptibility.

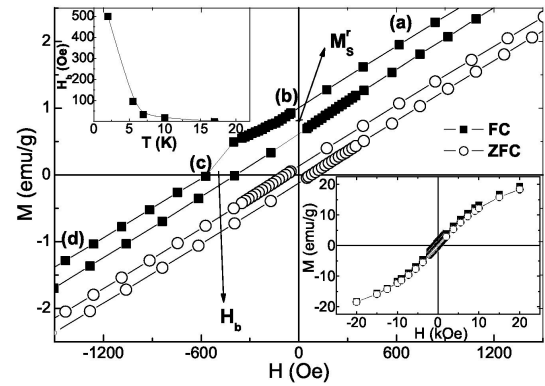


FIG. 3: Low-field section of the magnetization isotherms (in ZFC and FC modes) at $T = 2$ K. Top inset: thermal dependence of the bias $H_b(T)$ obtained from the FC $M(H)$ results. Bottom inset: $M(H)$ measured up to 20 kOe. (a), (b), (c) and (d) refer to Fig. 4 (see text).

the rise in $M_{FC}(T)$. The inset of Fig. 2 displays the out-of-phase component χ'' of ac susceptibility as a function of temperature under a magnetic field of 2 Oe and at frequencies $f = 0.5, 1, 3$ and 10 kHz. The results exhibit two maxima located at $T_{BB} = 45-55$ K and $T_f \sim 12$ K. The maximum at T_{BB} was associated to the blocking process of the superparamagnetic (SPM) magnetic moments in inner part of the HNS, hereafter (BULK). T_{BB} has a large dependence on frequency, which is an indication of the existence of a thermally activated process, with an energy barrier $E_a = 1.8 \times 10^{-13}$ erg. Assuming that E_a is the product $K_{eff}V_{BULK}$ (V_{BULK} is estimated from Mössbauer experiments as will be discussed later on), we obtain $K_{eff} = 1.3 \times 10^6$ erg/cm³ for this phase, slightly higher than bulk magnetite. The second maximum at T_f hardly change with frequency and we associated it to

the freezing of a cluster-glass like phase (CGP) structure in the disordered uncompensated surface regions (outer surface S_1 and inner surface S_2). The rise of the ZFC and FC magnetization showed in Fig. 2 could be associated to the uncompensated magnetic moment at the surface, which will provide an increase of the ferrimagnetic moment below T_f . Fig. 3 shows a detail of the magnetization loops measured in the ZFC and FC (cooling field $H = 10 \text{ kOe}$). We observed a large "loop shift" in FC cycle when measured at temperatures below the CGP freezing temperature ($T_f < 20 \text{ K}$). The bias field, H_b , is defined as the center field of the shifted magnetic loop. Usually, in "core-shell" nanoparticles, H_b is associated to the bias anisotropy induced by the "exchange interaction" between the magnetic microstructures in the frustrated ordered shell pinned by a large surface magnetic anisotropy and the soft ferromagnetically ordered core of the particle [2, 8]. In our case, we should understand the origin of this bias field considering that the nanoparticles are not "core-shell" but hollow nanospheres with two surface layers (S_1 and S_2) and the BULK inner region, as represented in figure 4. In principle we can assume that S_1 and S_2 regions are highly frustrated magnetic layers of magnetic clusters with a large surface magnetic anisotropy (responsible for the low temperature freezing of the surface magnetic moments, T_f). The inner BULK region shows a SPM behavior with low magnetic anisotropy. When cooling the sample down to 2 K under an external applied magnetic field H_0 , the resultant magnetization along the applied field direction will be the sum of the contribution of the surface regions (\vec{M}_S) and the BULK (\vec{M}_B): $\vec{M} = \vec{M}_S + \vec{M}_B$ in the HNS (a). Once the field is removed (b) at 2 K (below T_f), the freeze magnetic moments will keep a remanent magnetization (\vec{M}_S^r , see hysteresis loop of Fig. 3). We will consider that \vec{M}_S is contributed by \vec{M}_S^r , which is pinned during the whole hysteresis cycle, and \vec{M}_S^{up} , which is the unpinned field induced component at the surface ($\vec{M}_S = \vec{M}_S^r + \vec{M}_S^{up}$). When we apply an external magnetic field opposite to the magnetization direction (c), the magnetization within the BULK will rotate at low field values (soft phase) but the freeze magnetic moments at S_1 and S_2 will retain the magnetic state in which were frozen \vec{M}_S^r . This process will reduce \vec{M} reaching $M = 0$ at $\vec{H}_0 = -\vec{H}_b$, where $\vec{M}_B = -\vec{M}_S$. The field necessary to compensate \vec{M}_S^r is the responsible of the "bias field" (see Figure 4). Increasing H_0 an increase of the magnetization is obtained favoring an alignment of the magnetic moments along the H_0 in opposite direction to the (a) and (b) situation. Increasing H_0 in the opposite direction of the cooling field, we can reach the situation depicted in (d), which is almost symmetric to (a). However, \vec{M}_S^r contribution remains and is the responsible for the shift of the hysteresis loop toward positive values of magnetization when H_0 is again reduced. \vec{M}_S^r is originated in the FC process be-

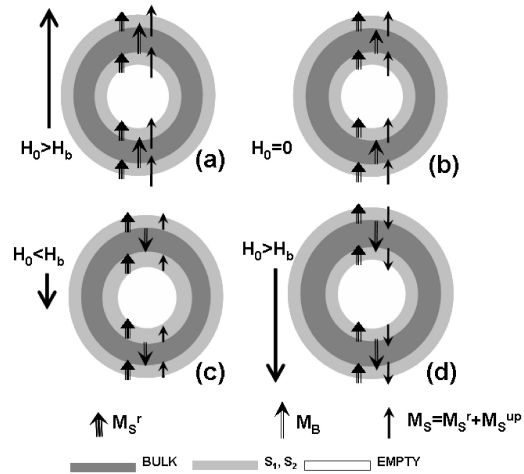


FIG. 4: Schematic representation of the magnetization process of the sample after FC below T_f . (See explanation in the text).

low T_f and it is absent when the sample is ZFC. Thus, H_b disappears for temperatures above T_f or ZFC due to random alignment in the CGP (M_S^r).

Mössbauer spectra (MS) were taken at 4.2-300 K in a liquid He flow cryostat with a conventional constant-acceleration spectrometer in transmission geometry using a $^{57}\text{Co}/\text{Rh}$ source. For in-field measurements, the powder sample was mounted in a vertical source-sample-detector setup in the bore of a 140 kOe superconducting magnet, such that the direction of γ -ray is parallel to the applied field. The spectra were fitted by using Lorentzian line shapes, and a foil of $\alpha - \text{Fe}$ was used to calibrate the velocity scale. The room-temperature MS spectrum is a doublet with narrow lines (line width $w = 0.65 \text{ mm/s}$), $IS = 0.36 \text{ mm/s}$ and quadrupolar splitting $QS = 0.98 \text{ mm/s}$. The IS value is similar to what is commonly observed in nanostructured ferrites in SPM regime [9]. However, the QS value, which originates in the local charge density symmetry, is much larger than the expected for these materials, reflecting a local symmetry lower than cubic, which in turn will break the Fe-Fe superexchange paths and/or oxygen vacancies located at both inner and outer surfaces. This is consistent with the picture of a magnetically disturbed spin configuration at the surface [10]. At 4.2 K (Fig. 5-a) the relaxation time is slow enough to ensure a static hyperfine splitting, and the spectrum could be fitted with two sextets associated to sites A and B in the spinel-type crystalline lattice. The obtained hyperfine field values ($B_{hf} = 491$ and 455 kOe for sites A and B, respectively) are smaller than bulk values [11], an effect usually observed in core-shell struc-

tures and assigned to the small E_a (and the associated softening) for the collective magnetic excitations which act to reduce the hyperfine fields with respect to their values at $T = 0 K$ [12]. However, in our case the E_a value is of the same order than observed for crystalline magnetite nanoparticles. Thus, the origin of reduced B_{hf} is the surface disorder. The large linewidth values of the magnetic sextets (Fig. 5-a) also indicate a locally disordered environment of Fe ions. In MS experiments under applied field, the effective hyperfine field B_{eff} will be the vector sum of the applied field H_{app} and the hyperfine field B_{hf} . Because of the strong antiferromagnetic interaction between sublattices A and B in the ferrites, B_{eff} of the sub-lattice A increases while B_{eff} of the sub-lattice B decreases. Moreover, the relative intensities of the six-line MS spectra are given by: $3 : p : 1 : 1 : p : 3$, $p = 4 \sin^2 \alpha / (1 + \cos^2 \alpha)$, where α is the angle between the spin and the gamma-ray direction [13]. Therefore, lines 2 and 5 vanish when the magnetic moments of the particles align to the applied field. Fig. 5-b shows the MS spectra measured at 4.2 K under $H_{app} = 120 kOe$, which is composed of very broad, strongly overlapping lines. Considering our TEM and magnetic data, we proposed a fitting procedure based on the combination of two crystalline sextets with narrow lines plus a continuous $P(B_{eff})$ distribution consistent with the existence of the (CGP). The crystalline sextets were assumed to correspond to spins in A and B sites aligned with applied field (red and blue subspectra, respectively). In addition, the intensities of lines 2 and 5 are fixed at 0 for these components. The relative area of these crystalline subspectra is 6-7 %, showing that only a small fraction of spins, probably located in the BULK region, are aligned to the external field. The hyperfine field distribution resulting from the fitting is displayed in the inset of Fig. 5-b, and it is associated to the sites not aligned with H_{app} . Its contribution amounts to 87 %, reflecting a high fraction of misaligned moments. If we consider that the surface moments are the only one disordered at high field, we can estimate a thickness of 0.9 nm for S_1 and S_2 regions and an inner diameter of 4 nm (empty region) compatible with STEM profile (see Fig. 1-d). The effective field distribution is very broad, with an equivalent probability for all B_{eff} values between those obtained for the two crystalline sextets. In addition, the ratio between the line 2 and 3 (I_{23}) for this component is very close to 2, the same as for a randomly oriented sample. This result supports the picture of a spatially disordered freezing of a large amount (87%) of spins residing in the morphologically disordered surface areas.

Summarizing, we propose a new synthesis method to obtain ferrite hollow nanospheres. The magnetic characterization of this type of nanostructures brings about relevant phenomena which are explained within a simple model based on the coexistence of a SPM soft phase (BULK) and the CGP hard phase (S_1 and S_2).

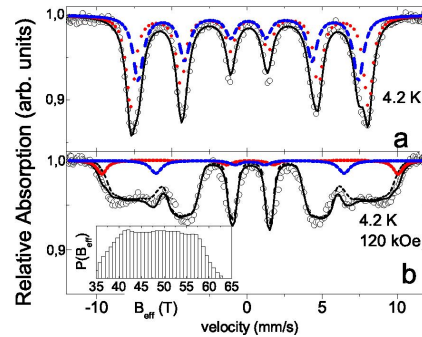


FIG. 5: Mössbauer spectra: a) Low temperature 4.2 K and b) under applied field ($H_{app} = 120 kOe$). Solid line is the fitted spectrum and dashed red and blue lines are the subspectra referent to sites A and B, respectively. Inset of figure 5-b is the hyperfine field distribution obtained from the fitting procedure.

We acknowledge the critical reading and discussion with Prof. P. A. Algarabel. This work received financial supported from Argentinian ANPCyT, CONICET and UNCuyo, Spanish MEC under grants: NAN2006-26646-E and Consolider CSD2006-12, and Brazilian FAPESP and CNPq. G. F. G. acknowledges support from the Spanish MEC through the Ramon y Cajal program. E. L. Jr. acknowledges fellowship by FAPESP.

-
- [1] M. Arruebo, R. Fernandez-Pacheco, M. R. Ibarra, J. Santamaría, *Nano Today* **2**, 23 (2007). G. F. Goya, V. Grazú, M. R. Ibarra, *Current Nanoscience* **4**, 1 (2008).
 - [2] B. Martinez, X. Obradors, L. I. Balcells, A. Rouanet, C. Monty, *Phys. Rev. Lett.* **80**, 181 (1998).
 - [3] X. Battle, A. Labarta, *J. Phys. D: Appl. Phys.* **35**, R15 (2002).
 - [4] R. H. Kodama, A. E. Berkowitz, *Phys. Rev. B* **59**, 6321 (1999).
 - [5] S. Peng, S. Sun, *Angew. Chem. Int. Ed.* **46**, 4155 (2007). A. Cabot, V. F. Puentes, E. Shevchenko, Y. Yin, L. Balcells, M. A. Marcus, S. M. Hughes, A. P. Alivisatos, *J. Am. Chem. Soc.* **129**, 10358 (2007).
 - [6] S. Sun, H. Zeng, D. B. Robinson, S. Raoux, P. M. Rice, S. X. Wang, G. Li, *J. Am. Chem. Soc.* **126**, 273 (2004).
 - [7] J. M. Vargas, R. D. Zysler, *Nanotechnology* **16**, 1474 (2005).
 - [8] R. D. Zysler, M. Vasquez Mansilla, D. Fiorani, *Eur. Phys. J. B* **41**, 171 (2004).
 - [9] G. F. Goya, T. S. Berquó, F. C. Fonseca, M. P. Morales, *J. Appl. Phys.* **94**, 9520 (2003).
 - [10] J. M. D. Coey, *Phys. Rev. Lett.* **27**, 1140 (1971).
 - [11] A. D. Arelaro, E. Lima Jr., L. M. Rossi, P. K. Kyohara, H. R. Rechenberg, *J. Magn. Magn. Mater.*, doi:10.1016/j.jmmm.2008.02.066
 - [12] S. Mørup, *J. Magn. Magn. Mater.* **37**, 39 (1983).
 - [13] D. P. E. Dickson, F. J. Berry (Eds.), "Mössbauer Spectroscopy", Cambridge University Press (1986), Chap. 4.